



CHAPTER III

RESEARCH METHODOLOGY

3.1 Testing Equipment

Equipments and specimens to be used, with the exemption of those to be used for image analysis, are in accordance with the specifications and other details stated in ASTM C 1579-06.

3.1.1 Specimen Molds

For the test specimen, a metal mold with a depth of 100 ± 5 mm and rectangular dimensions of 355 ± 10 mm by 560 ± 15 mm as illustrated in Figure 3.1 was used. A separate sheet metal piece shall seat snugly at the bottom of the mold with stress risers and internal restraints fabricated on it. Two 32 ± 1 mm risers are placed 90 ± 2 mm inward from each end of the mold to provide restraint in the concrete. There would be a 64 ± 2 mm stress riser at the center that would function as the initiation point for plastic shrinkage cracking. A sample of the existing specimen mold is shown in Figure 3.2.

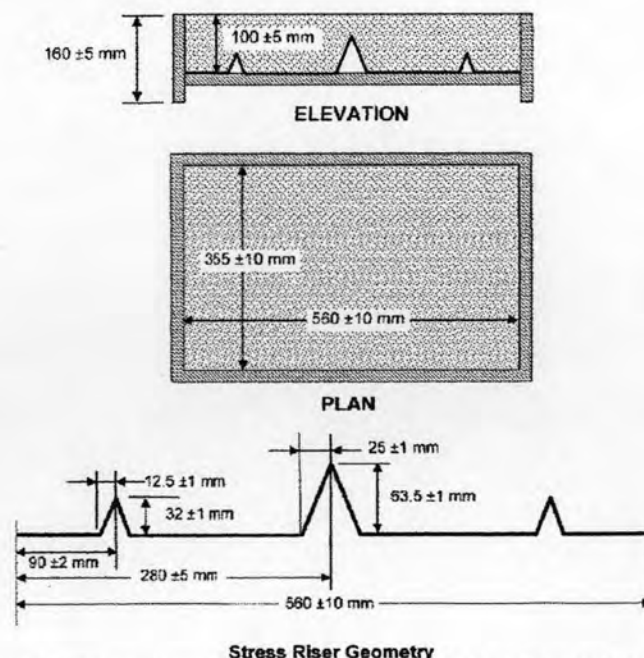


Figure 3.1: Specimen molds as specified in ASTM C 1579-06



Figure 3.2: Existing specimen molds built from specifications

3.1.2 Test Chamber

A preexistent test chamber, which was previously utilized for testing plastic shrinkage cracking of fiber reinforced concrete, was used. This chamber (Figure 3.5), though built based on the recommendations from the Acceptance Criteria for Concrete with Synthetic Fibers (AC32), was similar to the suggested sample set-ups (Figures 3.3 and 3.4) from ASTM 1579-06. The existing chamber had fans capable of blowing an average wind speed of 4m/s over the entire test panel situated at the end of each of the compartments. This set-up conformed to ASTM 1579-06 specifications since the fans, although having non-adjustable speed settings, was able to produce a uniform non-turbulent flow over the top surface of the specimen. However, blade-type heaters were installed next to the fans in order to be able to somehow control environmental conditions. Such arrangement allowed for heated air to be blown inside the chamber. The heaters had adjustable dial settings to permit adjustments, when necessary, during the experimental proper. Environmental conditions were monitored using an anemometer and hygrometer instead of having a built-in sensor. The test chamber allows for multiple slab panels to be tested having four available compartments for specimens and one compartment for the monitoring pan. A clear cover allows for easy observations during the testing period. A monitoring pan

suitable for exposing water in the air stream whose sides are vertical and expose at least $0.10 \pm 0.01 \text{ m}^2$ of water is required. The size of the pan will aid in the calculation of evaporation rate. The monitoring pan is placed on a scale for continuous monitoring and easy recoding of weight loss without removal during testing. The existing chamber set-up was able to efficiently produce the required $1.0 \text{ kg/m}^2 \cdot \text{h}$ minimum evaporation rate.

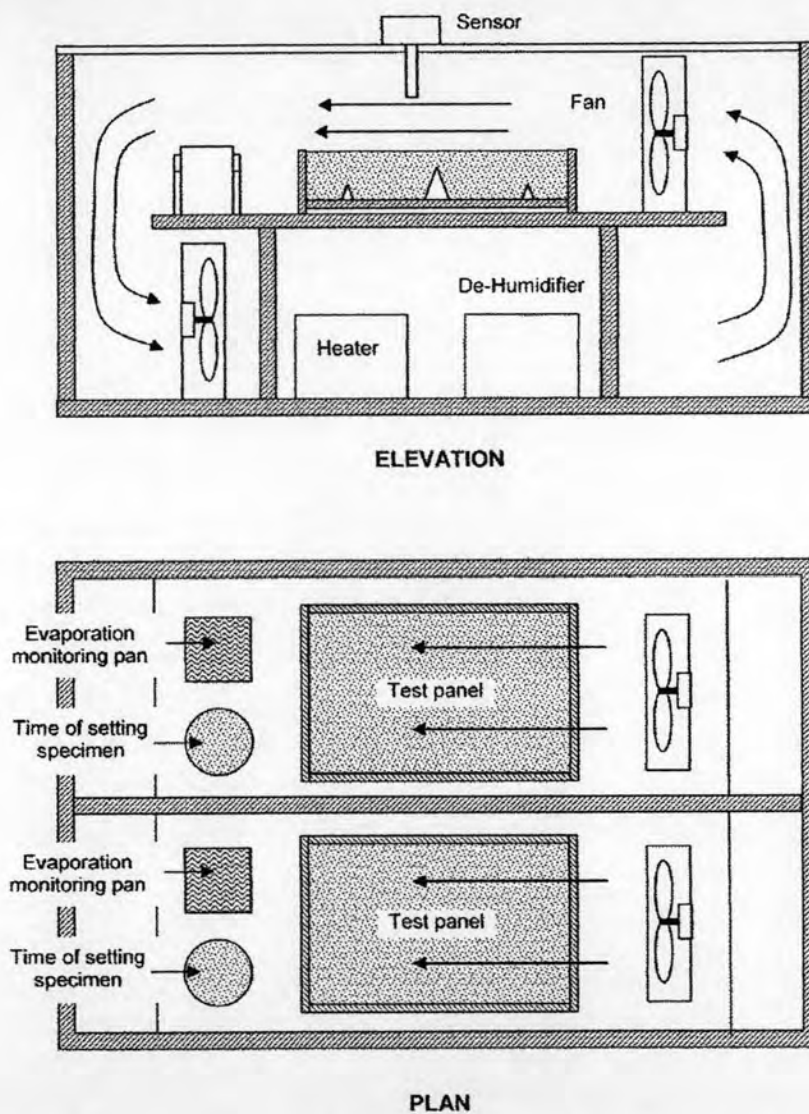


Figure 3.3.: Schematic setting of chamber to maintain environmental conditions (ASTM C 1579-06)

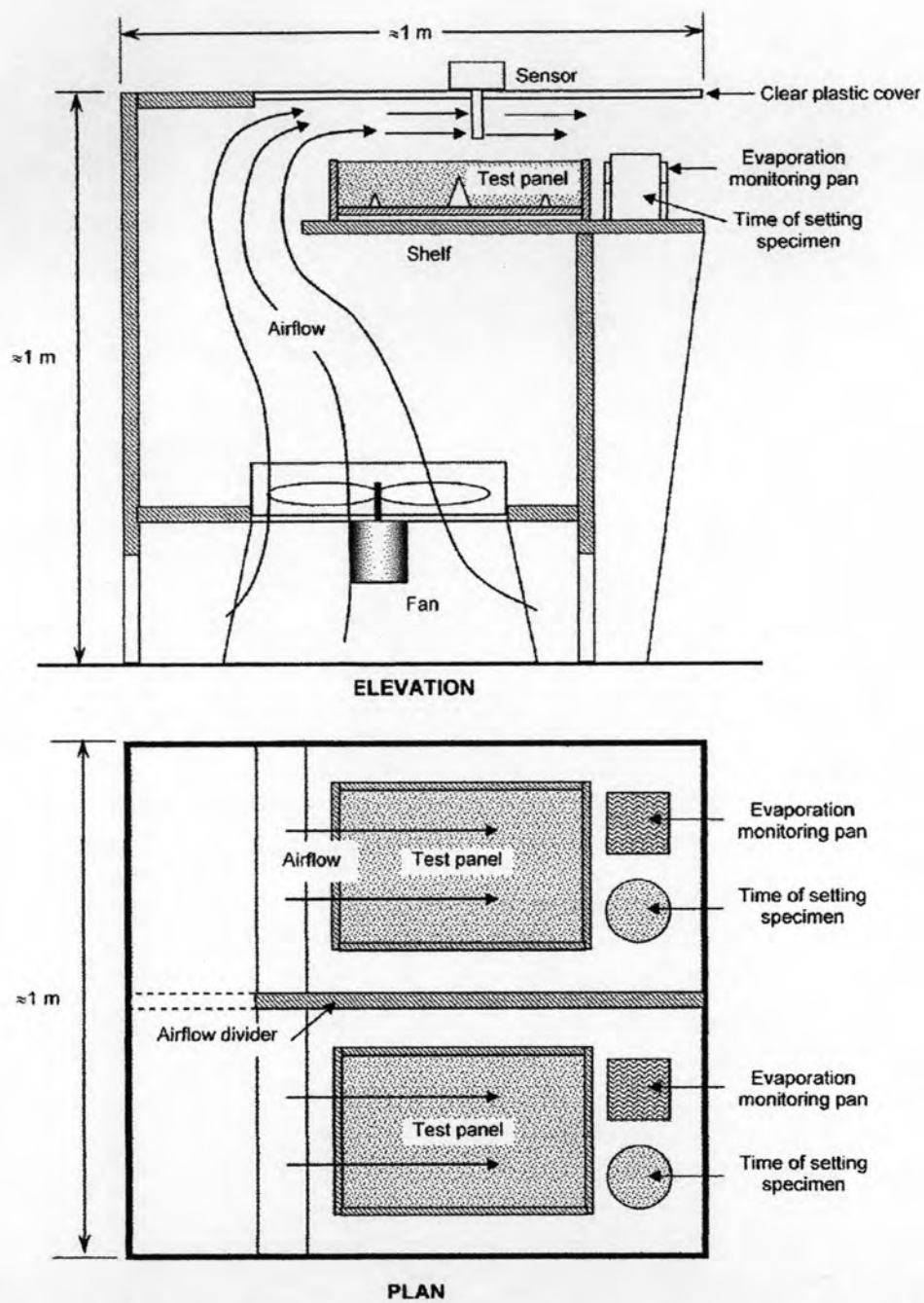


Figure 3.4: Schematic setting of fan box to maintain environmental conditions (ASTM C 1579-06)



Figure 3.5: Existing test chamber

3.1.3 Image Analysis Technique

Due to the emergence of digital technology, the use of the technique of Image Analysis evolved from the earlier methods of quantifying cracks such as using an optical hand-held microscope or a crack comparator. In essence, Image Analysis captures data in the least amount of time (or in real time such as in video recordings) and allows processing of acquired data by means of applicable programs. Generally, Image Analysis technique is separated into two parts: image capturing and image processing. This new technique basically requires the use of digital recording tools and imaging softwares. Digital recording tools were used to acquire data, such as in the form of digital images or videos, in only a matter of seconds. Imaging softwares aided in further manipulation and processing of recorded data.

Constant changes in technology allowed for the emergence of high resolution digital recording tools. The higher the resolution, the finer details could be captured. Accuracy, in this technique, would be measured in terms of how fine or detailed the

recorded data would be. In other words, the accuracy of the recording tool would be the minimum width (of the plastic shrinkage crack) that could be observed. Given the resolution of the recording tool, aspect ratio of the output image, and dimensions of the actual specimen to be observed, the accuracy could be calculated as

$$l = L_{eff} \times x_{spec} \quad (3.1)$$

$$w = W_{eff} \times y_{spec} \quad (3.2)$$

where, $L_{eff} = a \times L$

$$W_{eff} = a \times W$$

$$a^2(L \times W) = Pix_{total}$$

l = accuracy of the recording tool along the length of the observed specimen, mm

w = accuracy of the recording tool along the width of the observed specimen, mm

x_{spec} = actual length of the observed specimen, mm

y_{spec} = actual width of the observed specimen, mm

$(W_{eff} : L_{eff})$ = effective aspect ratio of the recording tool, pixel

$(W:L)$ = image aspect ratio, pixel.

a = percent effectiveness, %

Pix_{total} = resolution of the recording tool, pixel.

However, due to the curved nature of the lenses used in image capturing or recording, distortion occurs. In turn, the resulting images produce curved and not straight edges and some elements are possibly skewed. In this case, distortion also causes the image not be an exact replica of the original observed specimen. In essence, distortion would be determined when comparison is done such as between the observed specimen and its captured image. It is possible to make use of mathematical means in order to find a fitting representation of the comparison between the captured image and the original specimen such as by means of linear or nonlinear equations. It would be more reliable if the relationship between them would

be as close each other as possible so as to ensure the absence of distortion caused by the recording tool. In the process of comparison by means of mathematical equations, distortion would be in the form of residual error. Residual error is the measure of difference between the observed specimen and its captured image. The less the residual error, the less distortion there is. Sufficient softwares capable of doing such comparisons by finding the adequate mathematical representation with the least residual error would hasten this procedure.

Knowledge about the accuracy and distortion of the chosen recording tool measures the appropriateness or suitability of such tool for experimental use. From this information, proper measures could be done once applied in experimental testing.

It must be noted that apart from the distortion caused by lens curvature, additional distortion may occur due to the uneven ground surface where the specimen is placed or due to the uneven surface of the specimen observed. This type of distortion, caused by external factors other than the image recording tool itself, usually happens once the chosen recording tool is used in the experimental proper. If further analysis would be done from the captured image, then it is recommended that the image must be as close to the original specimen as possible. In this case, then image rectification would be done. Image rectification makes use of the predetermined mathematical equation (that was able to provide the least residual error), referred to as the transformation equation, to transform the geometry of the captured image into a fitted geometry and thus producing a rectified image. In concept, rectification would require the use of control points to serve as guides for the resulting output. The number of control points needed depends on the transformation equation. A higher order equation would require more control points. In addition to minimizing (if not eliminating) distortion, image rectification is useful in transforming image pixels into a chosen measurement unit of output. If done, numerical analysis of images could be done with convenience. Adequate softwares able to conduct image rectification might be used. Depending on the software used, transformations are usually done by statistical fitting means (such as least squares fit).

The abundance of available softwares for measurement means makes quantification by Image Analysis technique convenient. Measurement by any capable imaging software would primarily involve using the rectified image in determining the required quantities of the actual observed specimen. Since after image rectification the images are transformed with minimal error, then results of quantification would be more reliable to be as close as it could be to the original studied specimen. More advanced or enhanced imaging programs could possibly be able to quantify various details, depending on the research needs.

In this research, data in the primary form of pictures were taken of the test specimens with the use of a digital camera. A 10.1 MegaPixel digital camera was used in taking images of the specimens for the duration of the experiment proper. A metal rigid frame was used as a coordinate guide for the pictures taken. A sturdy steel stand (Figure 3.6) was utilized to assist in taking pictures at a constant height and camera position to maintain uniformity during testing.

Once images are taken and stored, image correction and analysis would be done using imaging freeware and software, HyperCube and AutoCAD. These imaging softwares used were chosen for this research on the basis of their ability to rectify captured images and the ability to measure the cracks from rectified images, respectively. HyperCube would allow correction of digital images and make sure that the images are relatively flat. AutoCAD was used as a means to measure the cracks from the corrected images. As technology progresses with time, more imaging softwares would be made available. The choice of software to be used may be chosen depending on research needs, reliability of result, and convenience for the user.

Image Analysis technique was chosen to be applied for its capability of permitting fast acquisition of images without disturbing the sample. Even after drying has already been completed, the cracks would still be fragile. Therefore, it is necessary to take extreme care when applying the crack comparator or the optical hand-held microscope methodology for measuring such cracks. These older manual measuring techniques were tedious and time-consuming whereas Image Analysis allows the use of technology to assist in the measuring process.



Figure 3.6: Steel stand for taking pictures

3.2 Testing Procedure

3.2.1 Test Preparations

3.2.1.1 Calibrations

3.2.1.1.1 Test Chamber Calibration

The test chamber was calibrated to primarily be able to determine which settings would be sufficient to allow a minimum value of $1.0 \text{ kg/m}^2\cdot\text{h}$ evaporation rate. Such calibration was done per chamber compartment to make sure that each compartment would have suitable environmental conditions for testing. Once calibrated, it would be assumed that the environmental conditions and evaporation rate would be nearly the same in all compartments of the test chamber. Since the fans blew a non-adjustable wind speed of 4m/s , the appropriate heater settings were determined in order to produce the required evaporation rate. In turn, changes in the heater setting would have corresponding effects in the temperature and relative humidity conditions in the test chamber.

Calibration in the test chamber was done by performing evaporation rate tests in each compartment. The monitoring pan placed on a calibrated weighing scale was filled with water. The exposed lip of the monitoring pan must not exceed more than 5mm above the water level. The initial weight of the monitoring pan was recorded and the heater was set at the lowest dial setting (marked as 30 in the dial). The fan

was turned on and the weight loss of the monitoring pan was recorded every 10 minutes for the entire test duration of one hour. The fan was momentarily turned off for not more than 15 seconds in order to properly take the weight readings. The average evaporation rate was determined after testing then the next chamber would be tested using the same procedure until all five compartments are tested. If the average evaporation rate calculated was lower than the $1.0 \text{ kg/m}^2\cdot\text{h}$ minimum evaporation rate, the evaporation rate test was repeated using the next higher heater setting. It was found that all chambers were able to produce the minimum $1.0 \text{ kg/m}^2\cdot\text{h}$ evaporation rate using 60-70 heater dial settings. This dial setting would be used during testing. It must be noted that this setting would differ depending on what type of heater is used.

3.2.1.1.2 Digital Camera Calibration

Calibration of the digital camera to be used in acquiring images was necessary in order to determine the accuracy and distortion of the camera. The accuracy would impart the capacity of the camera to clearly distinguish an element. For example, ASTM 1579-06 required an accuracy of at least 0.5 mm which would mean that crack widths with at least 0.5 mm would be visible in the acquired images. The higher the camera resolution, the better the accuracy would be. Distortion had to be checked since camera lenses are curved by nature which actually creates images with slightly curved edges, instead of straight ones. In the process of determining distortion, means of correcting such distortion would also be determined. The best suitable transform equation determined at the end of this process would correct distortions made by the camera used.

The accuracy of the digital camera was determined by dividing the specimen size (length and width) by the effective aspect ratio (length and width) of the camera. The product of the effective aspect ratio must not exceed the camera resolution. It was found that for a 10 MegaPixel digital camera with aspect ratio of 3:4 (3000:4000), the effective aspect ratio was 91% of the original 3:4 (2730:3640). Having a specimen size of 360 mm by 560 mm, it was found that the chosen camera has an accuracy of 0.15mm for length and 0.13 mm for width.

Distortion was checked by initially taking a sample picture. First, two grid patterns of 10 cm and 5 cm (using a good ruler as a standard) was drawn on a good quality paper having the same size as that of the test specimen. Taking the lower left corner to be the origin, the coordinates of each intersecting point (x_i, y_i) were noted in millimeters by manual measurement. A picture of the paper grid was taken on a relatively flat surface.

Using HyperCube, the coordinates of the intersecting points in the sample picture was determined through the Warp function of the program. These coordinates (x'_i, y'_i) are measured in pixels. The new set of coordinates are saved in a text file in *.pts format and edited (in either Microsoft NotePad or WordPad) to incorporate the two sets of coordinates (x_i, y_i) and (x'_i, y'_i) . The first two columns contained the coordinates in pixels (x'_i, y'_i) and the last two columns contained the coordinates in millimeters (x_i, y_i) . The first line of the text file stated the number of grid points (n) in the sample picture. In general, the format of the text file was:

n			
x'_1	y'_1	x_1	y_1
x'_2	y'_2	x_2	y_2
\vdots	\vdots	\vdots	\vdots
x'_n	y'_n	x_n	y_n

where $i = 1$ to n . In order to determine the distortion, these two sets of coordinates would be fitted into a series of mathematical equations in pairs (one for column coordinates and one for row coordinates). HyperCube uses least squares fit manner and produces the residual value which indicates the mean error of the fit. The mathematical equations used by HyperCube, called transformation equations, are listed in Table 3.1. A sample of the 10cm grid points is shown on Figure 3.7.

Table 3.1: List of HyperCube transformation equations

Transformation Equations	
Orthogonal	$ax + by + c$ (constraints on coefficients)
Affine	$ax + by + c$ (no constraints on coefficients)
Quadratic (4 terms)	$ax + by + cxy + d$
Quadratic (6 terms)	$ax + by + cxy + dx^2 + ey^2 + f$
Quadratic (8 terms)	$ax + by + cxy + dx^2 + ey^2 + fx^2y + gy^2x + h$
Cubic (8 terms)	$ax + by + cxy + dx^2 + ey^2 + fx^3 + gy^3 + h$
Cubic (10 terms)	$ax + by + cxy + dx^2 + ey^2 + fx^2y + gy^2x + hx^3 + iy^3 + j$
Projective (4)	$(ax + by + c)/(dx + ey + 1)$ for column
	$(fx + gy + h)/(dx + ey + 1)$ for row

Again, using the Warp function in HyperCube, the sample picture and text file of the coordinates were loaded. Once the text file was loaded, all coordinate points (from manual measurement and from HyperCube) would be seen as in Figure 3.8. The dark points (cross hair marks) along the grid are in pixels, the lighter ones are in millimeters.

File	Edit	Format	View	Help
B5				
89	2244	0	0	
669	2253	100	0	
1268	2254	200	0	
1880	2252	300	0	
2485	2245	400	0	
3089	2235	500	0	
3523	2224	574	0	
68	1645	0	101	
656	1647	100	101	
1259	1647	200	101	
1877	1643	300	101	
2492	1639	400	101	
3098	1632	500	101	
3538	1625	574	101	
50	1038	0	202	
644	1034	100	202	
1252	1030	200	202	
1873	1026	300	202	
2494	1024	400	202	
3102	1022	500	202	
3547	1021	574	202	
42	430	0	301	
638	420	100	301	
1246	411	200	301	
1868	406	300	301	
2493	404	400	301	
3102	406	500	301	
3548	408	574	301	
40	83	0	358	
636	68	100	358	
1244	57	200	358	
1866	50	300	358	
2492	50	400	358	
3100	53	500	358	
3547	57	574	358	

Figure 3.7: Ten cm grid points

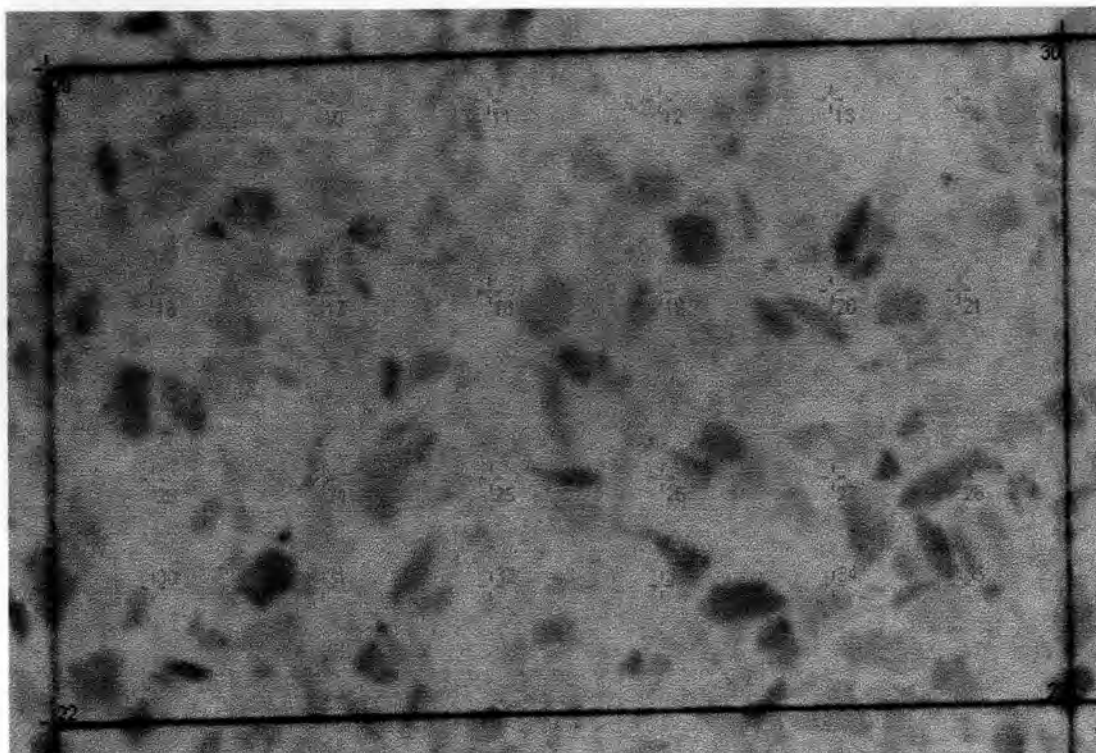


Figure 3.8: Control points of sample paper grid as shown in HyperCube Warp Function.

The Warp Function of HyperCube transforms the image units from pixels to millimeters. The best fitted mathematical equation that would transform the pixel coordinates into the millimeter coordinates was chosen based on the residual value that would emerge from performing the Warp function. The least residual value, the better the warped image would be (the image would be more flat).

Based on the calibration results from both the 10cm and 5cm sample picture, it was found that the best fit transform equation that suited the testing program was a Cubic-10 term equation ($ax + by + cxy + dx^2 + ey^2 + fx^2y + gxy^2 + hx^3 + iy^3 + j$). It produced the least residual of 1.98. This equation was used in the image correction of the images of the test specimens.



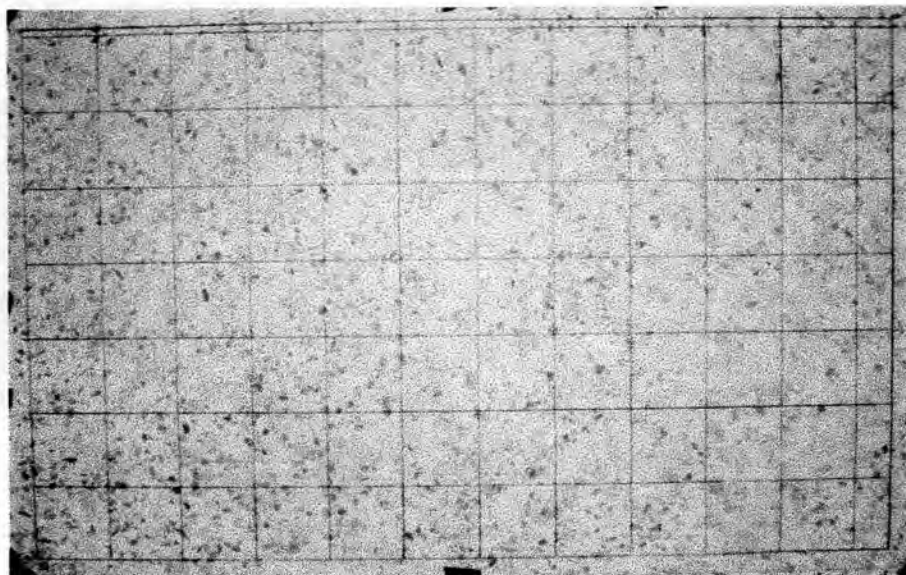


Figure 3.9: Original digital image of 5 cm grid paper for calibration

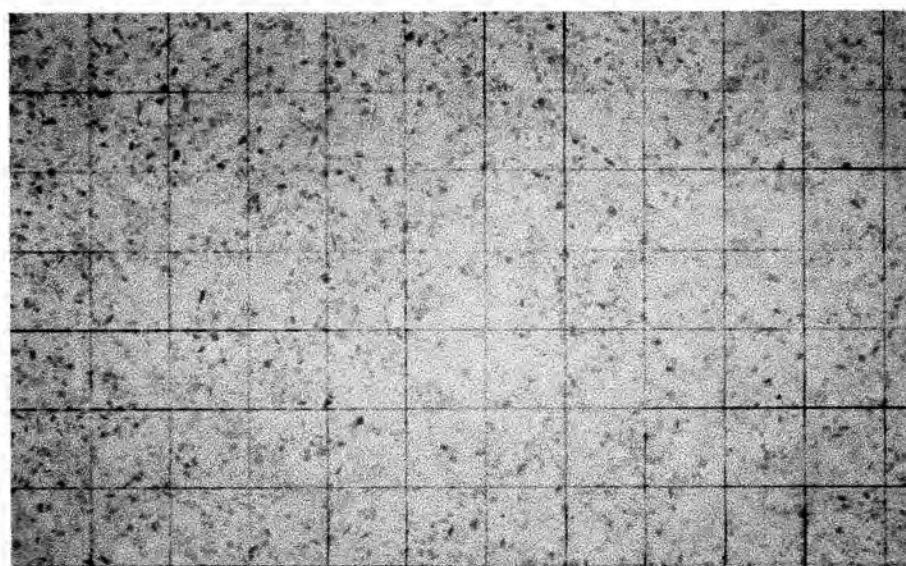


Figure 3.10: Corrected image of 5 cm grid paper using Cubic-10 term equation of the Warp function in HyperCube

3.2.1.2 Materials and Mix Design

ASTM Type I Portland cement was used for this study. The maximum size of crushed stone as coarse aggregate is 19 mm and has a specific gravity of 2.72. Fine aggregate used was natural sand with fineness modulus and specific gravity of 2.86 and 2.60, respectively. The gradation curves for both coarse and fine aggregates are shown in Figures 3.11 and 3.12, respectively. These gradation curves passed the

requirements in ASTM C 33-03. Mae Moh fly ash (found in Thailand) and silica fume in pellet form were used as pozzolan. The material properties and chemical composition (by percent of weight) could be seen in Tables 3.2 and 3.3, respectively. Chemical composition of the materials was done with the use of X-ray fluorescence (XRF) spectrometer.

Table 3.2: Material properties

Materials	Properties
Cement	Ordinary Portland cement Type I; specific gravity: 3.14;
Fly Ash	Mae Moh fly ash; specific gravity: 2.40; SiO ₂ : 48.06%
Silica Fume	Silica fume pellets; specific gravity: 2.20; SiO ₂ : 63.09%
Fine Aggregate	Sand; F.M.: 2.86; specific gravity: 2.60;
Coarse Aggregate	Crushed stone; specific gravity: 2.72

Table 3.3: Material chemical composition (% by weight)

Oxides	OPC Type I	Mae Moh Fly Ash	Silica Fume
SiO ₂	30.75	48.06	63.09
Al ₂ O ₃	11.05	30.05	27.74
Fe ₂ O ₃	1.37	5.46	3.28
CaO	49.21	10.02	2.14
MgO	< 0.01	0.05	0.84
K ₂ O	0.30	1.08	1.99
SO ₃	4.22	3.81	< 0.01

Gradation Curve for Coarse Aggregates

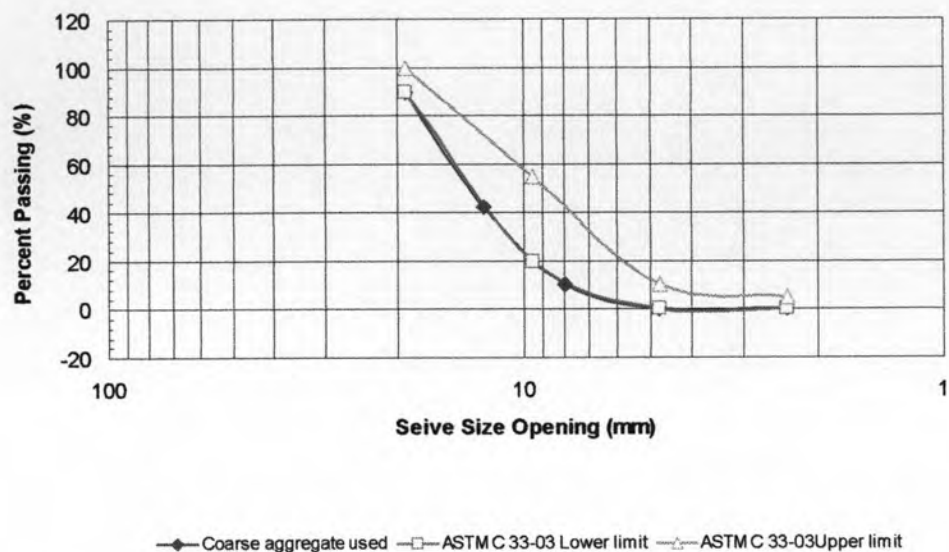


Figure 3.11: Gradation curve for coarse aggregate

Gradation Curve for Fine Aggregates

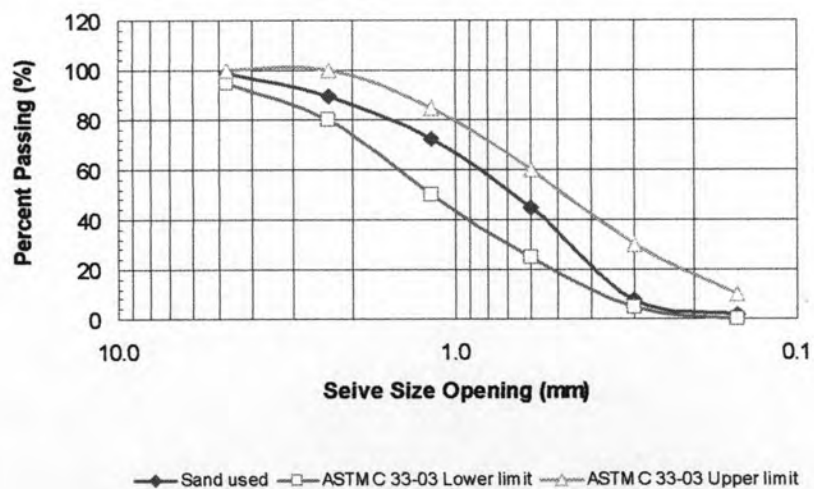


Figure 3.12: Gradation curve for fine aggregate

The fly ash replacements by weight of cement were at 10% increments from the range of 0 to 50. As for silica fume concrete mixes, replacements by weight used were 3% and 5%. The water/binder ratio was 0.30, 0.40, and 0.50. Silica fume concrete mixes only utilized 0.50 water/binder ratio. The mix proportion of concrete can be seen in Table 3.4.

Table 3.4: Primary mix design

Designation	w/b Ratio	Pozzolan Content	Content				
			Water	Cement	Pozzolan	Coarse Agg.	Fines
w/b-%FA/SF	-	-	kg/m ³	kg/m ³	kg/m ³	kg/m ³	kg/m ³
30-C	0.30	0.00	205	683	0	1024	472
30-10FA		0.10	205	615	68	1024	472
30-30FA		0.30	205	478	205	1024	472
30-50FA		0.50	205	342	342	1024	472
40-C	0.40	0.00	205	513	0	1024	613
40-10FA		0.10	205	462	51	1024	613
40-20FA		0.20	205	410	103	1024	613
40-30FA		0.30	205	359	154	1024	613
40-40FA		0.40	205	308	205	1024	613
40-50FA		0.50	205	257	257	1024	613
50-C	0.50	0.00	205	410	0	1024	698
50-10FA		0.10	205	369	41	1024	698
50-30FA		0.30	205	287	123	1024	698
50-50FA		0.50	205	205	205	1024	698
50-3SF		0.03	205	398	12	1024	698
50-5SF		0.05	205	390	21	1024	698

For each water/binder ratio, a control (C) mix was included as a means of comparison for the fly ash (FA) and silica fume (SF) concrete mixes. The amount of water as well as the amount of aggregates, both coarse and fine, was kept constant in the mix design. Only the amount of pozzolan used was varied in order to determine study the effect of pozzolan amount on the plastic shrinkage cracking of concrete.

3.2.1.3 Setting Time Tests

The initial and final setting times of the mixes studied were determined in accordance with ASTM C 403/C 403M-05. The mortar specimens were placed in the test chamber and exposed them to environmental conditions with a minimum evaporation rate of 1.0 kg/m²·h. The final setting time would dictate the duration of the plastic shrinkage cracking test.

3.2.2 Plastic Shrinkage Cracking Test

The main core of the testing procedure relies on the plastic shrinkage cracking test. This testing procedure would enable the quantification of the plastic shrinkage cracks that would emerge after exposure to environmental conditions in the test chamber.

As in ASTM C 1579-06, the test specimens are cast in the laboratory in accordance with the stated applicable provisions in ASTM C 192. For silica fume concrete, it was necessary to dry mix the pellet-form silica fume with aggregates for five minutes first in order to crush the pellets into powder to be more dispersed and uniformly distributed.

The panel molds were filled with fresh concrete using one layer. There were three specimens per concrete mix. The concrete was consolidated using external vibration until the top was approximately level with the top of the mold. After screeding and trowelling, the specimens were placed in the test chamber downstream from the fans. The monitoring pan was placed in one of the compartments to monitor the evaporation rate. The initial weight of the monitoring pan filled with water (the exposed lip of the monitoring pan must not extend more than 5 mm above the water level at the start of the test) was noted and the fans and heaters were turned on to obtain the required evaporation conditions. The evaluation of cracking commenced at this time.

At the start of the test and at 10-minute intervals, the air temperature, relative humidity, and weight of the monitoring pan were recorded. The weight of the monitoring pan was noted to the nearest 5 g, temperature to the nearest 0.50 °C, and relative humidity to the nearest 1%. The environmental condition readings were taken at a location 100 ± 5 mm above the panel surface. Required data was recorded until the time of final setting (determined in accordance with ASTM C 403/C 403M).

The evaporation rate was determined during each time interval by dividing the mass loss between successive recorded weights by the surface area of the water in the

monitoring pan and the time interval between each recording. The fans were briefly turned off to be able to take the readings from the weighing scale. Readings were taken not longer than 15 seconds so as not to disturb the test conditions in the chamber too much. Adjustments were made in the setting of the heaters, when required, in order to achieve the average evaporation rate of $1.0 \text{ kg/m}^2\cdot\text{h}$.

For every 30-minute interval from the start of the test until final setting time, the test panels are momentarily taken out of the test chamber to be able to take pictures of the specimens. The digital camera was situated on the metal stand and the stand was slid on top of the specimen. A metal rigid frame (the same size as the specimen) was placed on top of the panel whose picture was taken. The metal frame with 5 cm grid points at its inner edges would act as a guide in image correction by Image Analysis processing. The points on the edges of the metal frame were noted in millimeters (x,y). Three pictures were taken per specimen. The entire duration of taking pictures took approximately 1.33 minutes per panel (4 minutes for all three test specimens) for the entire process of taking the specimen out from the test chamber, taking digital images, and putting the specimen back into the test chamber to be completed.

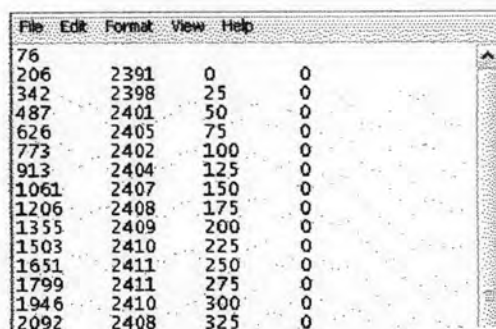
At the end of the test (when final setting time was reached), the atmospheric variables were recorded and the fans were stopped. Pictures of the test panels were taken and the weight of the monitoring pan noted. The average evaporation rate for the entire test duration was calculated. The test is not valid if the average evaporation rate is less than $1.0 \text{ kg/m}^2\cdot\text{h}$. ASTM 1579-06 allows for an allowance of -5% of the minimum average rate of evaporation.

After the testing duration, digital images of the test panels would undergo Image Analysis processing (explained in the next section) to determine the crack area, maximum crack width, average crack width, and cracking reduction ratio.

3.2.3 Image Analysis Processing

Image Analysis processing would assist in the quantification of plastic shrinkage cracks from the images captured earlier in the testing. Stored images of the test panels at the end of the test are loaded into HyperCube for image correction. Image correction was needed in order to minimize, if not eliminate, distortion.

As in the process used in calibrating the digital camera, the images (in JPEG format) are opened in HyperCube. Using the Warp function, the coordinates of the grid points of the metal frame were determined in pixels (x',y') and saved in a text file (in *.pts format). The saved text file and was edited (using Microsoft NotePad or WordPad) to incorporate the manually measured coordinates (x,y) in millimeters. The text file format of the two sets of coordinates from digital camera calibration was followed. The first line in the text file stated the number of control points measured. The first two columns contained the coordinates of the points in pixels (x',y') and the last two columns contained the coordinates of the points in millimeters (x,y).



76				
206	2391	0	0	
342	2398	25	0	
487	2401	50	0	
626	2405	75	0	
773	2402	100	0	
913	2404	125	0	
1061	2407	150	0	
1206	2408	175	0	
1355	2409	200	0	
1503	2410	225	0	
1651	2411	250	0	
1799	2411	275	0	
1946	2410	300	0	
2092	2408	325	0	

Figure 3.13: Example of control points in text file

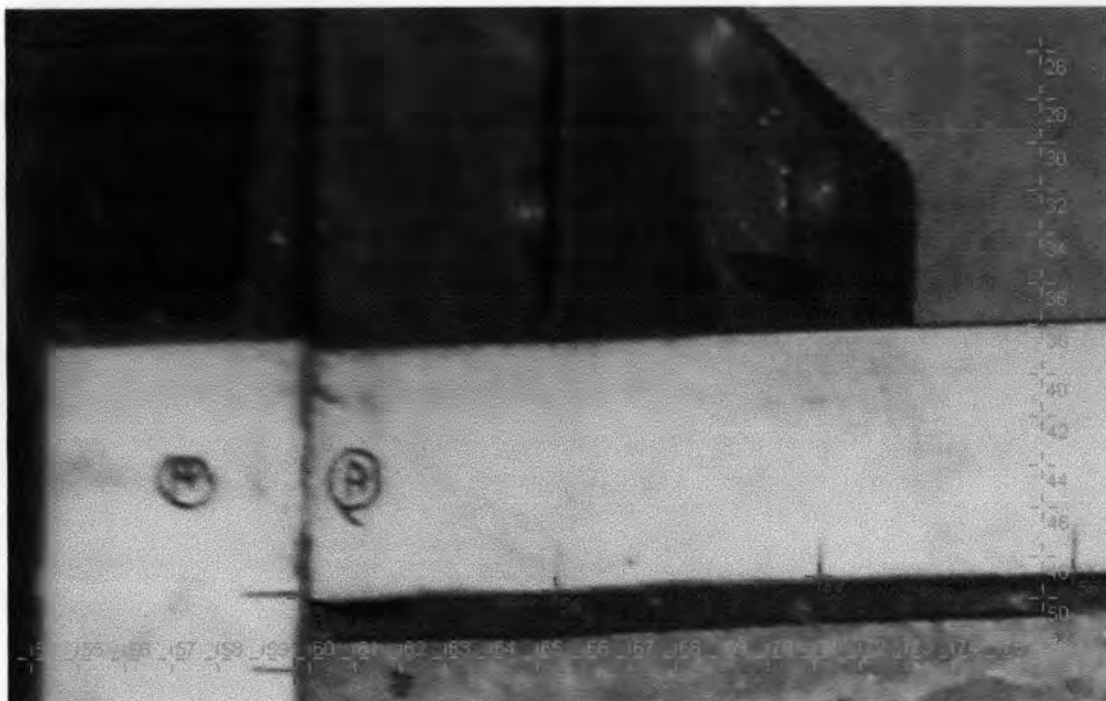


Figure 3.14: Control points of a test specimen as shown in HyperCube Warp Function.

Once editing was finished, the edited control points (that contained both sets of coordinate points in pixels and millimeters) and image to be corrected were once again loaded into the Warp function in HyperCube. The dark points along the inner edge of the frame are in pixels, the lighter ones are in millimeters. An example of which is shown in Figure 3.14. Using the predetermined Cubic- 10 term transform equation, the picture would be warped into a corrected image. The corrected image had noticeably straighter edges. A sample of an unaltered image and the resulting image after correction could be seen in Figures 3.16 and 3.17. The residuals of the corrected images using Cubic-10 terms transform equation were about 5 to 6. Such residual values were still acceptable meaning that the corrected image did not deviate too much from the original picture and was not distorted. The corrected picture was saved in TIFF format for further use in AutoCAD for the quantification of cracks. A more detailed example on the use of HyperCube for image rectification can be found at the appendix.

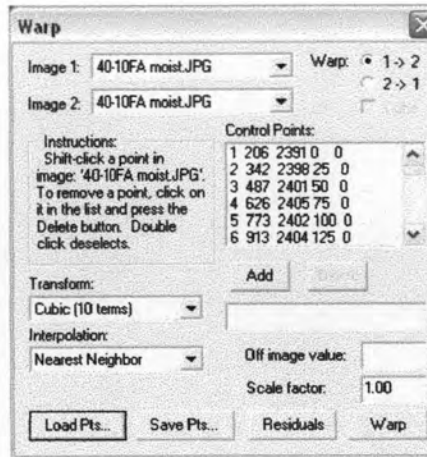


Figure 3.15: Warp function in HyperCube

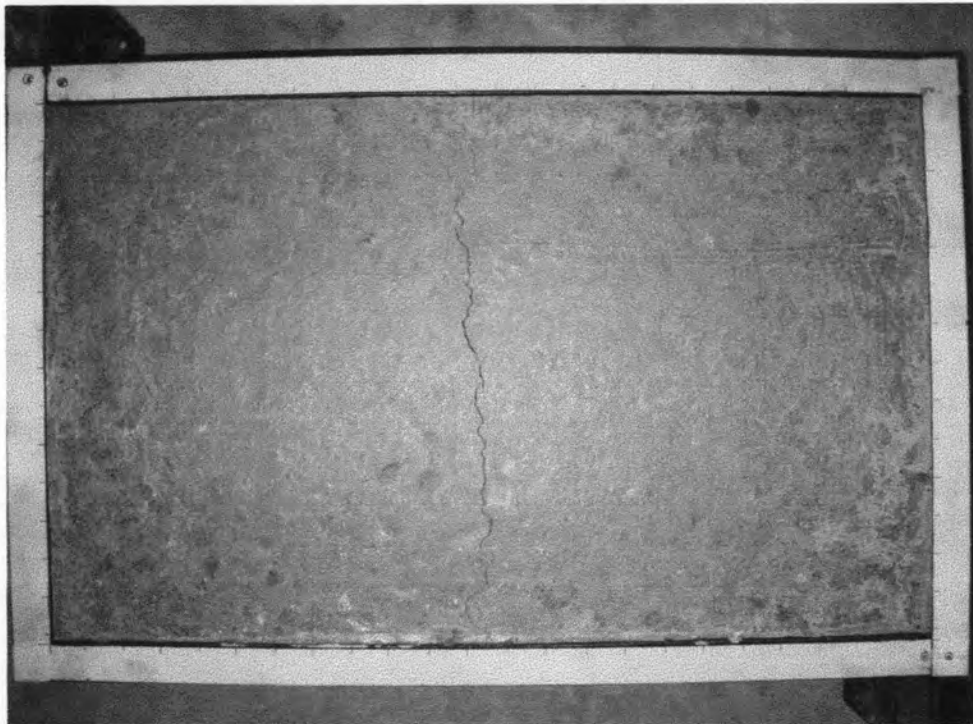


Figure 3.16: Original image of a 40-10FA specimen



Figure 3.17: Corrected image of a 40-10FA specimen using HyperCube

Using the corrected images from HyperCube, the amount of cracking was quantified using AutoCAD. The primary unit of measurement was set to millimeters. The images in TIFF format were loaded in AutoCAD and its dimensions were determined. Horizontal grid lines parallel to the longer side of the panel (perpendicular to the length of the crack) were made at an offset of 5 mm from the edge, as seen in Figure 3.18. These grid lines served as a guide in the measurement of crack width.

It was suggested in ASTM C 1579-06 that in order to avoid any possible effects of panel boundaries on crack width, the crack widths were not measured within 25 mm from the edge of the panel. The width of the crack was measured along the cracking path over the stress riser in a progressive order from one side to the other. Trial measurements at 1 mm intervals resulted in only differences of less than 1.50% in crack area, 0.45% in maximum crack width, and 0.60% in average crack width from the values attained from using 5 mm intervals. Therefore, the crack widths were chosen to be measured at 5 mm intervals along the crack.

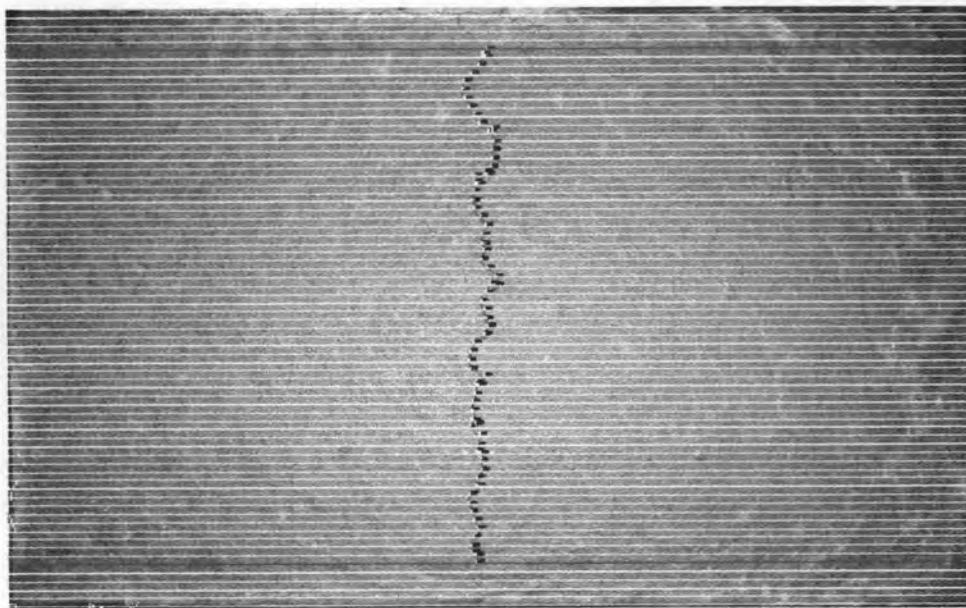


Figure 3.18: Measurement of crack widths along 5 mm grid lines using AutoCAD

3.2.4 Curing Procedure

In order to be able to determine the effect of curing on the plastic shrinkage cracks, chosen specimens would undergo different curing conditions. Comparison would be done after 28 days of moist curing by wet burlap and air curing in terms of the changes in values of crack area, maximum crack width, and average crack width.

After processing, the two panels with greater calculated crack area were chosen for further observation for 28 days under different curing conditions. From the chosen two panels, the one that had higher crack area was chosen for moist curing by wet burlap and the other for air curing.

After 28 days, digital images were taken and processed by Image Analysis once again. Crack area, maximum crack width, and average crack width were calculated. The percentage change of such values was also computed to be able to be able to see the effects of the different curing conditions applied to the chosen test specimens.

3.3 Quantification of Plastic Shrinkage Cracks

Plastic shrinkage crack quantification terms of crack area, maximum crack width, and average crack width would aid in properly analyzing the effect of pozzolan in the plastic shrinkage cracking of concrete.

The maximum crack width (in mm) was determined from the measured crack widths. The average crack width (in mm) was calculated as

$$\text{Average Crack Width} = \frac{\sum_{i=1}^n w_i}{n} \quad (3.3)$$

where, w_i = measured crack widths, mm

n = total number of measurements along the crack.

The area (in mm^2) for every 5 mm increment, since using 5mm increments had less than 1.5% difference in values from using 1 mm increments as discussed previously in section 3.2.3, was determined by multiplying the average crack width by the crack length (which is equal to the increment, 5 mm, in each section) as shown in the formula

$$\text{Area} = A_i = \left(\frac{w_i + w_{i+1}}{2} \right) \times l_i \quad (3.4)$$

where, $l_i = 5$ mm.

The crack area (in mm^2) was calculated as the summation of the area per section or simply the area of the entire measured crack.

$$\text{Crack Area} = \sum_{i=1}^n A_i \quad (3.5)$$

where, A_i = area calculated per section.

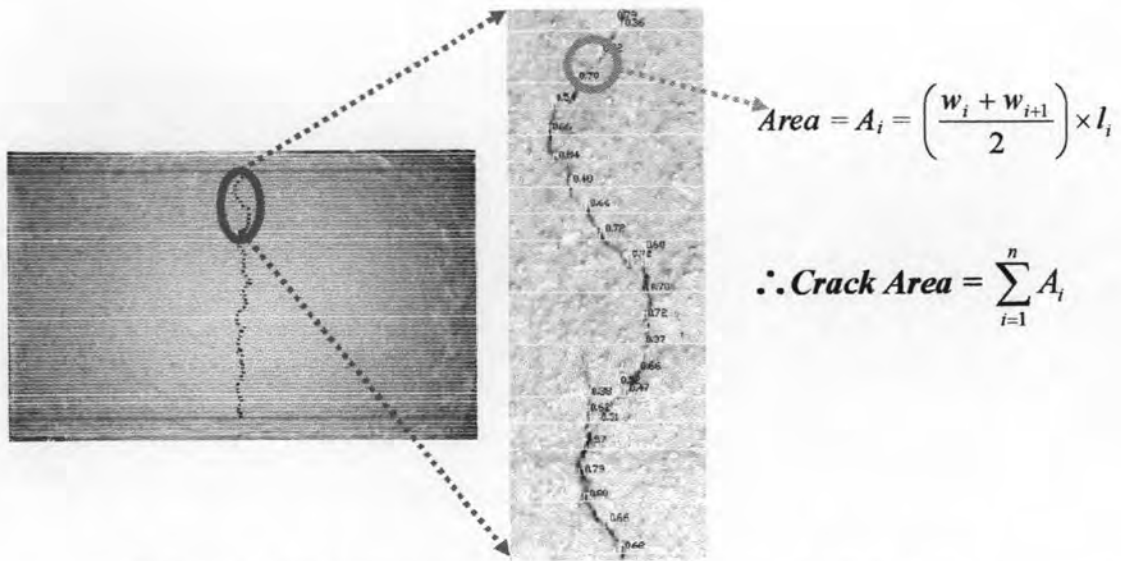


Figure 3.19: Determining crack area from measured crack widths

The cracking reduction ratio was calculated in order to determine the effectiveness of pozzolan in reducing plastic shrinkage cracks in terms of average crack width (ASTM 1579-06). The formula used was as follows,

$$CRR = \left(1 - \frac{w_{poz}}{w_{con}} \right) \times 100\% \quad (3.6)$$

where, CRR = cracking ratio with respect with the average crack width, %

w_{poz} = average crack width of the pozzolan specimen, mm

w_{con} = average crack width of the control specimen.. mm

Based on the formula shown, the cracking reduction ratio compares the calculated average crack width of the pozzolan specimen with respect to that of the control specimen. If the CRR value is positive, then it would show that the use of pozzolan would effectively reduce plastic shrinkage crack width. Essentially, greater the positive value of the calculated cracking reduction, the more effective the pozzolan is in reducing plastic shrinkage cracks.

After 28 days, the chosen specimens for curing (under moist curing and air curing conditions) were processed using Image Analysis once again. New values of crack widths from Image Analysis were used to determine the new set of values of maximum crack width, average crack width, crack area, and cracking ratio. The effect

of curing was determined by calculating the percentage change of the values from the first set crack quantification values as shown in the following formulas:

$$\% \Delta_{MW} = \left(\frac{MW_1 - MW_{28}}{MW_1} \right) \times 100 \quad (3.7)$$

$$\% \Delta_{AW} = \left(\frac{AW_1 - AW_{28}}{AW_1} \right) \times 100 \quad (3.8)$$

$$\% \Delta_{CA} = \left(\frac{CA_1 - CA_{28}}{CA_1} \right) \times 100 \quad (3.9)$$

where, $\% \Delta_{MW}$ = percent change of maximum crack width after 28 days, %

$\% \Delta_{AW}$ = percent change of average crack width after 28 days, %

$\% \Delta_{CA}$ = percent change of crack area after 28 days, %

MW_1 = initial maximum crack width after testing, mm

MW_{28} = maximum crack width after 28 days, mm

AW_1 = initial average crack width after testing, mm

AW_{28} = average crack width after 28 days, mm

CA_1 = initial crack area after testing, mm²

CA_{28} = crack after 28 days, mm²

The use of Microsoft Excel in tabulating measured crack widths and calculating required values was used for convenience. Essential graphs and statistical tools using SPSS for Windows were also used for analyses of the data acquired.